



Published in final edited form as:

*Adv Mater.* 2010 November 9; 22(42): 4754–4758. doi:10.1002/adma.201002767.

## A DNA Nanostructure-based Biomolecular Probe Carrier Platform for Electrochemical Biosensing

**Hao Pei,**

Laboratory of Physical Biology, Shanghai Institute of Applied Physics, Chinese Academy of Sciences, Shanghai, 201800 (P. R. China)

**Na Lu,**

Laboratory of Physical Biology, Shanghai Institute of Applied Physics, Chinese Academy of Sciences, Shanghai, 201800 (P. R. China)

**Yanli Wen,**

Laboratory of Physical Biology, Shanghai Institute of Applied Physics, Chinese Academy of Sciences, Shanghai, 201800 (P. R. China)

**Shiping Song,**

Laboratory of Physical Biology, Shanghai Institute of Applied Physics, Chinese Academy of Sciences, Shanghai, 201800 (P. R. China)

**Prof. Yan Liu,**

Department of Chemistry and Biochemistry & The Biodesign Institute, Arizona State University, Tempe, AZ (USA)

**Prof. Hao Yan, and**

Department of Chemistry and Biochemistry & The Biodesign Institute, Arizona State University, Tempe, AZ (USA)

**Prof. Chunhai Fan**

Laboratory of Physical Biology, Shanghai Institute of Applied Physics, Chinese Academy of Sciences, Shanghai, 201800 (P. R. China)

Hao Yan: hao.yan@asu.edu; Chunhai Fan: fchh@sinap.ac.cn

A critical challenge in surface-based biomolecular detection is the reduced accessibility of target molecules to probes arranged on a heterogeneous surface compared to probe–target recognition in homogeneous solution.<sup>[1–5]</sup> To improve the recognition abilities of such heterogeneous surface probes, much effort has been devoted to control the surface chemistry, conformation, and packing density of the probe molecules as well as the size and geometry of the surface.<sup>[6–11]</sup> Here, we devise a new concept to achieve improved probe–target recognition properties by introducing a probe bearing a 3D DNA nanostructure-based chip platform. DNA nanotechnology has attracted intense interest because the unparalleled self-recognition properties of DNA offer flexibility and convenience for the ‘bottom-up’ construction of exquisite nanostructures with high controllability and precision.<sup>[12–20]</sup> Our strategy to design and construct 3D nanostructured recognition probes on a surface provides

a significantly enhanced spatial positioning range and accessibility of the probes on a surface over previously reported linear or stem-loop probe structures.<sup>[2,7]</sup>

While DNA hybridization in homogeneous solutions is generally rapid and specific, the confinement of DNA probes at solid surfaces often sacrifices such recognition properties to some extent.<sup>[3,21,22]</sup> However, sequence recognition at surfaces is a necessity for the development of low-cost and miniaturized field-portable DNA sensors. A large portion of reported DNA sensors are constructed on the basis of a classic, linear DNA probe-based two-step assembly strategy.<sup>[23]</sup> It involves self-assembly of thiolated single-stranded (ss-)DNA probes on planar gold surfaces by Au-S chemistry, followed by passivation with an alkanethiol (e.g., mercaptohexanol, MCH) that backfills the unoccupied space and forces the probe DNA to adopt an upright surface orientation that favors DNA hybridization.<sup>[23]</sup> Nevertheless, new strategies are needed to better control the inter-probe and probe-target interactions on surfaces.

In this work, we designed a DNA tetrahedron structure with pendant probe DNA at one vertex and three thiol groups at the other three vertices. Much recent progress has been made in developing 3D DNA architectures.<sup>[17,24–29]</sup> In particular, the ‘pyramidal’ DNA tetrahedra structures, which have proven to have mechanical rigidity and structural stability, are excellent candidates to anchor biomolecules on surfaces.<sup>[30]</sup> This 3D nanostructure is expected to be readily and strongly anchored at Au surfaces by the three thiols at the base of the ‘pyramid’, leaving a free-standing probe at the top (Figure 1a). This tetrahedron was hierarchically assembled from three thiolated DNA fragments of 55 nucleotides (55-nt) and one probe-containing DNA fragment of 80-nt, which were mixed in stoichiometric equivalents in buffer, heated, and then rapidly cooled to 4 °C. Of note, the tetrahedron assembly process was extremely fast (within 2 min) with a high yield of over 85% (one major band was resolved during electrophoresis), suggesting that the additional sequences and thiol groups did not significantly interfere with the assembly. Control studies showed that the tetrahedron moved more slowly than either the ssDNA or any other combinations lacking one or two strands, confirming the successful assembly of the nanostructure (Figure S1, Supporting Information).

Tetrahedron-structured probes (TSPs) can be self-assembled onto Au surfaces by their thiol groups (Figure 1a), as monitored in real time by a surface-sensitive acoustic method, quartz crystal microbalance (QCM) (inset of Figure 1b). Parallel QCM and surface plasmon resonance (SPR) evaluation suggested that a large amount of water was trapped within the thin TSP film due to the high capacity of the hollow tetrahedral structure (see Figure 1 and detailed analysis in the Supplementary Information, SI). The presence of the tetrahedral structure at Au surfaces was further confirmed by fluorescent studies (Figure S2, Supporting Information). TSPs labeled with a tetramethylrhodamine (TAMRA) dye at the top vertex exhibited stronger fluorescence at the Au surface, while non-thiolated tetrahedra led to essentially no fluorescence after rinsing with water, which confirms that TSPs are anchored at Au by thiol groups. We also labeled TSPs with TAMRA at one of the bottom vertices, the fluorescence of which was much weaker than TSPs with TAMRA distal to the surface. This difference can be attributed to the gold-induced, distance-dependent fluorescence quenching.<sup>[31]</sup>

The tetrahedral structure is a highly rigid scaffold<sup>[24]</sup> that accommodates DNA probes with well-defined probe-to-probe spacing. SPR provided a surface density estimate of  $4.8 \times 10^{12}$  TSP  $\text{cm}^{-2}$  (or  $8.0 \text{ pmol cm}^{-2}$ ) which, in combination with the tetrahedron size calculation, allowed us to estimate an inter-probe spacing of  $\sim 4.0 \text{ nm}$ . This TSP-based surface provides a reliable platform for the detection of DNA hybridization by a range of transducers (acoustic, optical, and mechanical). The TSP hybridization process was monitored both by QCM and

SPR in real time, producing comparable hybridization signals (Figure 1b, c). While TSP carries high negative charges that may serve as a barricade for target hybridization, we found that the hybridization efficiency could reach at least 80% as estimated from the QCM frequency change, suggesting that the high negative charges could be effectively screened in solutions with high ionic strength. In a study implementing a nanomechanical microcantilever setup,<sup>[32]</sup> the sequence-specific DNA hybridization was similarly reflected by the deflection of a micro-fabricated silicon cantilever coated with gold, while control sequences induced minimal deflection (Figure 1d).

While it is simple to construct sensors with real-time and label-free features, it is important to develop portable, user-friendly devices for point-of-care diagnostics. Electrochemistry is particularly suited to the development of DNA sensors since electrochemical detectors tend to pose low cost, mass, power, and volume requirements.<sup>[7,33–35]</sup> TSP-modified Au surfaces were amenable for electrochemical interrogation despite the presence of a relatively thick layer of TSPs (Figure 2a). To evaluate the viability of constructing an electrochemical DNA sensor using TSP-decorated gold electrodes, we first analyzed the electron-transfer reactivity at the TSP-conjugated surface since it has a much thicker layer (the structure of TSP plus a six-carbon spacer theoretically forms an ~6 nm layer) than the conventional ssDNA probe-based ones (a six-carbon spacer forms a layer of ~1 nm). Interestingly, we found that a redox molecule, 3,3',5,5'-tetramethylbenzidine (TMB), exhibited well-defined redox peaks at the TSP-modified surfaces (Figure S3, Supporting Information), which were significantly better than those at the much thinner 11-carbon alkane thiol-modified surfaces (~1.5 nm), suggesting that TMB could easily penetrate the hollow structures comprising the TSP layer.

Sensor performance was first evaluated by a direct detection mode employing biotinylated target DNA. The DNA hybridization event was transduced to electrochemical signals through the specific binding of an avidin-HRP (horseradish peroxidase) conjugate to the biotin, which leads to enzyme turnover-based signal transduction.<sup>[36,37]</sup> The presence of nanomolar quantities of target DNA led to a significant increase in amperometric signals corresponding to the catalytic reduction of H<sub>2</sub>O<sub>2</sub>, while no signal change was observed for even a large excess (micromolar) of non-cognate DNA sequences (Figure 2b). The amperometric signal increased non-linearly with the logarithmic concentration of the target, with a detection limit of at least 1 pM (>3 SD, standard deviation).

We note that this 1 pM sensitivity could be further improved by incorporating more advanced signal amplification methods (e.g., with nanomaterial-based amplification<sup>[8,38]</sup>). However, even this TSP-based sensor without rigorous signal amplification has been considerably more sensitive than ssDNA probe/MCH-based sensors with similar HRP-based signal transduction, exhibiting a 250-fold improvement in sensitivity (1 pM vs. 250 pM<sup>[36]</sup>). We attribute this improvement to the consistently favorable orientation of TSP at the Au surface, which avoids possible complications that are often encountered by soft ssDNA probes, e.g., entanglement between probes or local aggregation of the self-assembled monolayer (SAM).<sup>[39]</sup> Also interestingly, while MCH passivation is a critical step for the fabrication of linear DNA probe-based DNA sensors, TSP-modified electrodes, free of the passivation step, produced comparably large amperometric signals to those treated with MCH (Figure 2c). This effect was ascribed to the high rigidity of TSP<sup>[24]</sup> that allows it to stay at the Au surface with highly ordered upright orientation. In contrast, linear probes tends to lie flat at the surface in the absence of MCH treatment, leading to low hybridization efficiency.<sup>[2]</sup> Indeed, we find that a MCH treatment step can improve the amperometric signal for 1 nM target DNA by 20-fold with a linear probe-based sensor (Figure 2c).

Single nucleotide polymorphisms (SNPs) represent promising disease markers because they are stably inherited sequence variations in the human genome. Importantly, we found that

TSP-based DNA sensors possess remarkable selectivity for single-base mismatches (Figure 3a). The SNP discrimination factors between a fully complementary (A:T) and three internal single-base mismatched (T:T, C:T, G:T) targets were 150, 1000, and 10 000, respectively (Figure 3b). Such differences reflect the thermodynamic stability of each mismatch. Parallel studies with ssDNA probe-based sensors showed much poorer selectivity, with SNP discrimination factors of 6, 17, and 100, respectively. We suggest that both the profound nanometer-scale control of the inter-probe spacing and the reduced surface effects attributable to the presence of a thick TSP layer contribute to the greatly enhanced selectivity of TSP-based sensors over ssDNA probe-based ones.<sup>[37]</sup>

It is important to test the TSP-based electrochemical DNA sensor in complicated biological fluids (e.g., serum) in order to evaluate its real applicability. We employed SPR to interrogate the protein adsorption ability of Au surfaces modified with MCH, TSP, and a well known protein-resistant molecule, oligo(ethylene glycol) (OEG) thiol (Figure S6). Interestingly, while only the OEG surface showed complete resistance to bovine serum albumin (BSA) adsorption, the amount of BSA adsorbed at the TSP surface was considerably lower than at the MCH surface (~1/4). Additional studies with hemoglobin adsorption also revealed only minimal protein adsorption (Figure S6). This relatively high protein-repelling ability of the TSP surface permits the use of TSP-based sensors directly in serum. DNA hybridization assays are performed by a popularly employed 'sandwich' detection mode that is suitable for detection of label-free targets. An unlabeled target DNA is flanked by the capture probe and a biotinylated reporter probe that can bind to avidin-HRP. Significantly, we found that the TSP sensor was highly resistant to serum, with little alteration of the background noise and nearly the same hybridization signal for the 100 pM target, even in the presence of 50% serum (Figure S7).

Consequently, we believe that TSP-based surfaces may provide a versatile platform for the detection of a broad range of biomolecules by the combination of aptamers.<sup>[40–42]</sup> As a straightforward extension of DNA sensors, we replaced the DNA probe with an anti-thrombin aptamer sequence,<sup>[42]</sup> at the top of the tetrahedron, and assembled the aptamer-based TSP (aTSP) on Au surfaces, as we did with TSP. The aTSP-modified electrodes were deployed to electrochemically detect thrombin, a potential tumor marker, by using a biotinylated, paired aptamer that bound to a different domain and sequence of thrombin (Figure 4a). This aTSP sensor exhibited excellent sensitivity toward thrombin, with a remarkable detection limit of 100 pM (Figure 4b), which is lower than the ssDNA aptamer-based sensors by three orders of magnitude.<sup>[42]</sup>

In summary, we have reported a DNA tetrahedron-based platform for immobilization of nucleic acid probes on gold surfaces. The 3D DNA nanostructure-based electrochemical probe system provides several unique features, which led to a significantly improved performance compared to the conventional approaches of creating probes on heterogeneous surfaces. First, the TSP can be rapidly and reliably prepared with high yields, and readily assembled on gold surfaces in a single step with ordered orientation, well-controlled spacing, and high stability. More significantly, probes are separated from the surface by a relatively thick TSP layer, thereby placing them in environments that resemble their solution-phase counterparts<sup>[37]</sup> while still being amenable to electrochemical transduction. These properties are directly translated into high detection sensitivity and excellent sequence specificity (e.g., greatly enhanced SNP typing ability). Second, TSP-based sensors can be directly employed in detection in biological fluids because of the high protein resistance ability. Third, TSP-based surfaces are fully compatible with various acoustic, optical, mechanical, and electrochemical transductions, providing opportunities to develop various DNA-based sensors and nanodevices. In addition, TSP sensors are amenable to aptamer-based assays, which may provide a highly versatile platform for the detection of virtually

any target.<sup>[40,43]</sup> Given these advantages, we believe this DNA nanostructure-based TSP platform may become a new paradigm in biosensor design and significantly further the field of chip-based biomolecular detection.

## Experimental Section

All oligonucleotides were synthesized and purified by TaKaRa Inc. (Dalian, China), and the sequences are shown in Table S1. The TMB substrate (Neogen K-blue low activity substrate) was from Neogen (U.S.A.). Avidin-HRP was from Roche Diagnostics (Mannheim, Germany). All solutions were prepared with Milli-Q water (18 M $\Omega$  cm resistivity) from a Millipore system. Experimental setup and detailed procedures for electrochemistry, QCM, SPR, and cantilever are provided in the Supporting Information.

## Supplementary Material

Refer to Web version on PubMed Central for supplementary material.

## Acknowledgments

This work was supported by National Natural Science Foundation (20725516, 20873175, 90913014 and 21028005), Ministry of Science and Technology (2007CB936000), Ministry of Health (2009ZX10004-301), and SMCST(0952nm04600). H.Y. acknowledges funding from NIH, ONR, ARO, NSF, DOE, and Sloan Research Foundation. H.Y. was supported as part of the Center for Bio-Inspired Solar Fuel Production, an Energy Frontier Research Center funded by the U.S. Department of Energy (DE-SC0001016).

## References

1. Heller MJ. *Annu Rev Biomed Eng.* 2002; 4:129. [PubMed: 12117754]
2. Levicky R, Herne TM, Tarlov MJ, Satija SK. *J Am Chem Soc.* 1998; 120:9787.
3. Wong ELS, Chow E, Gooding JJ. *Langmuir.* 2005; 21:6957. [PubMed: 16008409]
4. Irving D, Gong P, Levicky R. *J Phys Chem B.* 2010; 22:7631. [PubMed: 20469913]
5. Wong IY, Melosh NA. *Biophys J.* 2010; 98:2954. [PubMed: 20550908]
6. Ricci F, Zari N, Caprio F, Recine S, Amine A, Moscone D, Palleschi G, Plaxco KW. *Bioelectrochemistry.* 2009; 76:208. [PubMed: 19362061]
7. Fan C, Plaxco KW, Heeger AJ. *Proc Natl Acad Sci USA.* 2003; 100:9134. [PubMed: 12867594]
8. Zhang J, Song S, Wang L, Pan D, Fan C. *Nat Protoc.* 2007; 2:2888. [PubMed: 18007624]
9. Soleymani L, Fang ZC, Sargent EH, Kelley SO. *Nat Nanotechnol.* 2009; 4:844. [PubMed: 19893517]
10. Li D, Song S, Fan C. *Acc Chem Res.* 2010; 43:631. [PubMed: 20222738]
11. Gong P, Levicky R. *Proc Natl Acad Sci USA.* 2008; 105:5301. [PubMed: 18381819]
12. Seeman NC. *Nature.* 2003; 421:427. [PubMed: 12540916]
13. Yan H. *Science.* 2004; 306:2048. [PubMed: 15604395]
14. Lin C, Liu Y, Yan H. *Biochemistry.* 2009; 48:1663. [PubMed: 19199428]
15. Lin CX, Katilius E, Liu Y, Zhang JP, Yan H. *Angew Chem Int Ed.* 2006; 45:5296.
16. Lin CX, Rinker S, Wang X, Liu Y, Seeman NC, Yan H. *Proc Natl Acad Sci USA.* 2008; 105:17626.
17. Sharma J, Chhabra R, Cheng A, Brownell J, Liu Y, Yan H. *Science.* 2009; 323:112. [PubMed: 19119229]
18. Zhang Z, Wang Y, Fan C, Li C, Li Y, Qian L, Fu Y, Shi Y, Hu J, He L. *Adv Mater.* 2010; 22:2672. [PubMed: 20440702]
19. Winfree E, Liu F, Wenzler L, Seeman NC. *Nature.* 1998; 394:539. [PubMed: 9707114]
20. Rothmund PW. *Nature.* 2006; 440:297. [PubMed: 16541064]

21. He S, Song B, Li D, Zhu C, Qi W, Wen Y, Wang L, Song S, Fang H, Fan C. *Adv Funct Mater.* 2010; 20:453.
22. Liu G, Sun C, Li D, Song S, Mao B, Fan C, Tian Z. *Adv Mater.* 2010; 22:2148. [PubMed: 20376817]
23. Levicky R, Herne TM, Tarlov MJ, Satija SK. *J Am Chem Soc.* 1998; 120:9787.
24. Goodman RP, Schaap IAT, Tardin CF, Erben CM, Berry RM, Schmidt CF, Turberfield AJ. *Science.* 2005; 310:1661. [PubMed: 16339440]
25. He Y, Ye T, Su M, Zhang C, Ribbe AE, Jiang W, Mao CD. *Nature.* 2008; 452:198. [PubMed: 18337818]
26. Andersen ES, Dong M, Nielsen MM, Jahn K, Subramani R, Mamdouh W, Golas MM, Sander B, Stark H, Oliveira CLP, Pedersen JS, Birkedal V, Besenbacher F, Gothelf KV, Kjems J. *Nature.* 2009; 459:73. [PubMed: 19424153]
27. Dietz H, Douglas SM, Shih WM. *Science.* 2009; 325:725. [PubMed: 19661424]
28. Douglas SM, Dietz H, Liedl T, Högberg B, Graf F, Shih WM. *Nature.* 2009; 459:414. [PubMed: 19458720]
29. Ke YG, Lindsay S, Chang Y, Liu Y, Yan H. *Science.* 2008; 319:180. [PubMed: 18187649]
30. Mitchell N, Schlapak R, Kastner M, Armitage D, Chrzanowski W, Riener J, Hinterdorfer P, Ebner A, Howorka S. *Angew Chem Int Ed.* 2009; 48:525.
31. Strohsahl CM, Miller BL, Krauss TD. *Nat Protoc.* 2007; 2:2105. [PubMed: 17853865]
32. Fritz J, Baller MK, Lang HP, Rothuizen H, Vettiger P, Meyer E, Guntherodt HJ, Gerber C, Gimzewski JK. *Science.* 2000; 288:316. [PubMed: 10764640]
33. Drummond TG, Hill MG, Barton JK. *Nat Biotechnol.* 2003; 21:1192. [PubMed: 14520405]
34. Patolsky F, Lichtenstein A, Willner I. *Nat Biotechnol.* 2001; 19:253. [PubMed: 11231559]
35. Wang J, Xu D, Polsky R. *J Am Chem Soc.* 2002; 124:4208. [PubMed: 11960439]
36. Carpini G, Lucarelli F, Marrazza G, Mascini M. *Biosens Bioelectron.* 2004; 20:167. [PubMed: 15308218]
37. Liu G, Wan Y, Gau V, Zhang J, Wang L, Song S, Fan C. *J Am Chem Soc.* 2008; 130:6820. [PubMed: 18459781]
38. Zhang J, Song S, Zhang L, Wang L, Wu H, Pan D, Fan C. *J Am Chem Soc.* 2006; 128:8575. [PubMed: 16802824]
39. Steel AB, Levicky R, Herne TM, Tarlov MJ. *Biophys J.* 2000; 79:975. [PubMed: 10920027]
40. Liu J, Cao Z, Lu Y. *Chem Rev.* 2009; 109:1948. [PubMed: 19301873]
41. Zuo X, Song S, Zhang J, Pan D, Wang L, Fan C. *J Am Chem Soc.* 2007; 129:1042. [PubMed: 17263380]
42. Xiao Y, Lubin AA, Heeger AJ, Plaxco KW. *Angew Chem Int Ed.* 2005; 44:5456.
43. Ellington AD, Szostak JW. *Nature.* 1990; 346:818. [PubMed: 1697402]

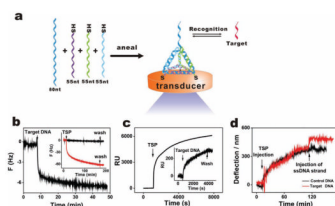


**Figure 1.**

Construction of a three-dimensional DNA nanostructure-based platform. a) Schematic representation of the construction of a TSP (tetrahedron-structured probe). The TSP was hierarchically assembled from three thiolated 55-nt DNA fragments and one 80-nt DNA fragment carrying the probe sequence, mixed in stoichiometric equivalents in buffer. This nanostructure is expected to readily anchor at the Au surface through three thiols at the base of the ‘pyramid’, leaving a free-standing probe at the top. b–d) Self-assembly process and hybridization with target are monitored in real-time using a quartz crystal microbalance (QCM) (acoustic), surface plasmon resonance (SPR) (optical), and a micro-cantilever (mechanical), respectively. b) Target hybridization process (QCM). Inset: the assembly process of TSP, the red and black curves represent TSP with or without thiol groups. c) The assembly process of TSP (SPR). Inset: the target hybridization process. d) The assembly and target hybridization processes (micro-cantilever), the red and black curves represent hybridization with complementary and non-complementary sequences, respectively.

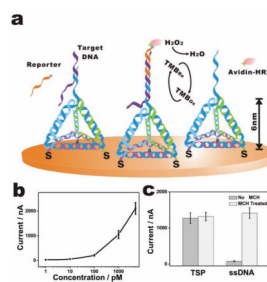


**Figure 2.**

TSP-based DNA electrochemical sensor. a) The presence of target DNA is transduced to electrochemical signals by the specific binding of an avidin-HRP (horseradish peroxidase) conjugate to the biotin label of the reporter probe and the resultant catalyzed electro-reduction of hydrogen peroxide in the presence of an electroactive cosubstrate, TMB, which offers high enzyme-based signal amplification. b) Amperometric measurements in the presence of target DNA at 1 pM, 10 pM, 100 pM, 1 nM, and 5 nM with the sandwich mode. c) Comparison of TSP and ssDNA probe-based sensor performance with or without MCH passivation (with 1 nM target DNA).



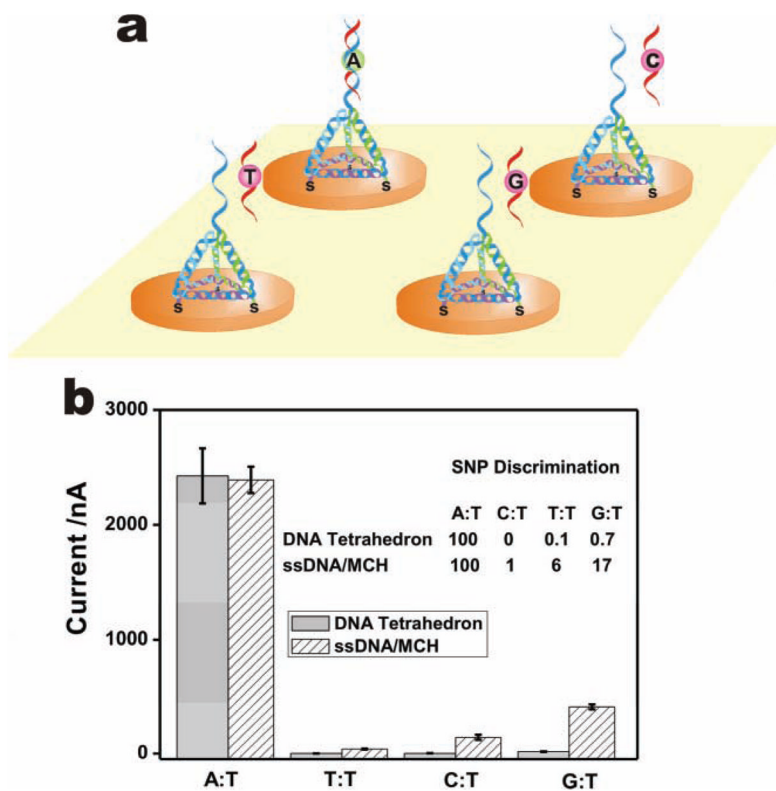


**Figure 3.**

a) Scheme for SNP detection with TSP. b) Comparison for the single-base mismatch discrimination ability of a TSP-based sensor and a ssDNA/MCH-based sensor for different mutant types. All target concentrations are 1 nM.

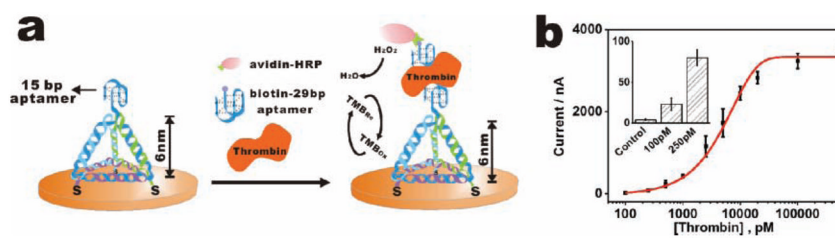


**Figure 4.** A TSP-based platform for the detection of proteins. a) aTSP-based thrombin detection scheme. b) Amperometric results for aTSP-based thrombin sensor. Inset: amperometric detection of thrombin in the low concentration range.